
# Transmembrane fluxes during electrolysis in high salinity brines: effects on lithium and other raw materials recovery

César H. Díaz Nieto , Matías A. Mata , Camilo J.O. Palacios , Noelia A. Palacios , Walter R. Torres , María L. Vera , Victoria Flexer

PII: S0013-4686(23)00579-0
DOI: https://doi.org/10.1016/j.electacta.2023.142401
Reference: EA 142401

To appear in: *Electrochimica Acta*

Received date: 1 March 2023
Revised date: 11 April 2023
Accepted date: 11 April 2023

Please cite this article as: César H. Díaz Nieto , Matías A. Mata , Camilo J.O. Palacios , Noelia A. Palacios , Walter R. Torres , María L. Vera , Victoria Flexer , Transmembrane fluxes during electrolysis in high salinity brines: effects on lithium and other raw materials recovery, *Electrochimica Acta* (2023), doi: https://doi.org/10.1016/j.electacta.2023.142401

# Transmembrane fluxes during electrolysis in high salinity brines: effects on lithium and other raw materials recovery

César H. Díaz Nieto, Matías A. Mata, Camilo J. O. Palacios, Noelia A. Palacios[†], Walter R. Torres[†], María L. Vera, **Victoria Flexer[†,*]**

Centro de Investigación y Desarrollo en Materiales Avanzados y Almacenamiento de Energía de Jujuy-CIDMEJu (CONICET-Universidad Nacional de Jujuy). Av. Martijena S/N, Palpalá, 4612, Argentina.

*Corresponding author: Victoria Flexer: vflexer@unju.edu.ar

[†]ISE MEMBERS

**ABSTRACT**

During the production of high purity lithium salts, magnesium and calcium will readily crystalize as either carbonates or hydroxides if their concentrations have not been depleted to below 2 ppm. Magnesium and calcium can be fully abated electrochemically by production of hydroxide anions via water electrolysis. While brine alkalization within an electrochemical reactor has shown great performance at proof-of-concept level, this is not feasible at industrial scale. Solids cannot be produced, nor accumulated within a water electrolyzer, and membrane fouling must be avoided at all costs. An alternative is to work on a brine that has been fully depleted from multivalent cations and produce an increase in pH beyond the needs for successful crystallization of the hydroxides. In this way, the super alkaline brine can be used as an external precipitating agent that does not dilute the other key components of the brine, namely lithium cations. We have studied the competing ion migration between chloride and hydroxide anions across an anion exchange membrane in a water electrolyzer as a function of current density. The most important differences were observed in the magnitude of the changes in the solution volumes. While water electrolysis and electro-osmotic effects were identified as processes contributing to these changes, only classical osmosis is responsible for the differential effects. In the range of study, applied current density values from 80-225 A $m^{-2}$ produced higher hydroxide concentrations, although no current density values were identified to produce remarkable changes in the energy efficiency. Beyond pH 14, the passage of hydroxide across the membrane becomes faster than that of chloride.

## 1. Introduction

Lithium has become a critical raw material for the fabrication of rechargeable lithium-ion batteries.[1,2] Today, lithium is mined from both hard rock ores and continental brines. While the largest share of current production comes from the former, the worldwide lithium resources in brines are much more abundant than in hard rock ores, and thus it is expected that in the medium to long term a larger share of production will come from brines.[3] When we refer to continental brines, we are referring to underground reservoirs within salt lakes or salars, where lithium ions are normally found in concentrations between 500 to 1500 ppm.[4,5] These continental brines are the only lithium rich aqueous sources in large scale exploitation today.[3] Though more diluted, lithium can also be found in other types of brines, such as geothermal deposits, or produced waters from the oil and gas industries, typically in concentrations ranging from 10 – 200 ppm.[6,7]

The currently available technology for the exploitation of lithium rich aqueous sources is known as the evaporitic technology. This archaic methodology largely relies on brine concentration in open air ponds. Brines must lose not less than 90% of their original water content so that $Li^+$ becomes more concentrated and the ratio of concentrations for $Li^+/Na^+$ becomes much higher.[4,5] Successful open air brine concentration requires an initial concentration of not less than 400 ppm $Li^+$, flat and inexpensive land around the deposits, and very scarce rains, so that ponds do not get refilled. These conditions are only met in very few deposits worldwide. Thus more diluted sources are not currently under commercial exploitation.[4,5] There is, however, widespread interest in developing technologies that will allow for their processing, both because of the increasing lithium demand, and because those more diluted brines are more widespread worldwide.[5,8–10]

Interest in overcoming the limitations of the current technology for lithium brine processing has paved the road for the proposal of many alternative technologies, collectively known as Direct Lithium Extraction Technologies (DLE). These comprise many different physico-chemical principles,[5] including some very promising electrochemical ideas.[11–13] Collectively, the main limitation of all DLE is their much higher energy cost.[5,14] It will evidently be extremely difficult to beat the low operational costs of open air evaporation. The putatively high operational costs associated to electrochemical technologies are often argued to directly discard these in favour of other DLE, such as ion exchange resins, the leading competitor in the DLE field.[4,5]

Lithium is a most interesting case study. A critical raw material strongly associated with renewable energies and sustainable mobility, it would be a huge inconsistency if lithium brine mining and processing would be associated to non-sustainable practices. The evaporitic technology is more and more often criticized due to the huge water volumes that are lost through evaporation.[15–17] However, some DLE approaches often leave many open questions regarding the sustainability of their potential large scale implementation, most notably due to the large fresh water volumes that would be required during processing.[5,18] For a full sustainability analysis any prospective brine processing methodology must be analysed from the overall mining perspective. Fresh water is always available in a laboratory, ready to be used in technology development, but might be an extremely limited resource next to mineral deposits. Likewise, waste management and disposal should also be considered. Finally, all lithium rich brines, be them continental, geothermal, or produced waters, are much more concentrated in co-existing ions than in $Li^+$.[4,5] Thus, these brines are an enormous opportunity for harvesting many more raw materials, including some critical

ones, such as magnesium.[5] In the circular economy[9,19] perspective, research on processing old mine tailings for the production of pure new products, different than the ones that were originally mined is a very active field.[20–22] The same applies to resource recovery from waste brines from desalination plants.[23–25]

Within the circular economy perspective outlined above, we have recently proposed an overall electrochemical approach for the joint recovery of lithium carbonate and several by-products.[26–30] Our idea, schematized in Figure 1a employs four different water electrolyzers fitted with both anion exchange and cation exchange membranes. In the first stage, brine is made alkaline by direct production of hydroxide anions in the cathodic compartment of a water electrolyzer, where multivalent cations are crystallized as hydroxides. In a typical continental brine, we are able to produce $Mg(OH)_2$ and $Ca(OH)_2$.[28] Next, a large fraction of $Na^+$ cations are crystallized as $NaHCO_3$, which can be directly converted to $Na_2CO_3$.[26] In the final step, $Li_2CO_3$ is produced.[27] In all three steps, we can alternatively produce either HCl or $Cl_2$. $H_2$ and $O_2$ are the obvious products of water electrolysis which could potentially serve for recovering, in a fuel cell, some of the energy originally invested.

Electromembrane approaches for the abatement of $Mg^{2+}$ cations are plentiful, based either on charge selective membranes,[31–33] or monovalent selective membranes.[34–38] The full abatement of divalent species is key for the ideas shown in Figure 1a, and for many other DLE approaches. Less well-known are electromembrane processes for the recovery of lithium salts, and these usually require lithium selective membranes[39] or extensive pre-processing.[40] The system shown in Figure 1a is evidently based on the well-established electrochemical principles of electrodialysis, the novelty is in their application to a new and highly complex chemical system.[41] Most $Li^+$ rich brines have total salinity values of 3-4 M, with $Li^+$ the most diluted species, not

representing more than 1 % of the total ionic content. Thus, developing all steps depicted in Figure 1a is key for the final successful recovery of lithium carbonate.

Electromembrane processes in general avoid at all costs membrane fouling by solid formation. The chlor-alkali process, as an example, employs NaCl solutions with multivalent ions' concentrations in the order of ppb.[42,43] One of the keys to develop the process schematized in Figure 1a is to look for ways to avoid solid formations within electrolyzers in general, and particularly in the vicinity of ion exchange membranes. One such strategy, schematized at the centre-left of Figure 1a, entails the use of a first batch of native brine, introduced in a *sacrificial electrolyzer* where divalent cations are fully depleted. The supernatant is then flowed towards another electrolyzer, and the solution is made further alkaline, so that it can be used as a precipitating agent in an external vessel.[30]

In work reported here, we aim at identifying the physico-chemical phenomena pertaining to the potential large scale implementation of this technology. We have worked with artificial alkaline NaCl brines (3.1 M NaCl) and we have studied the competing migration across an anion exchange membrane of hydroxide and chloride anions from pH 13 to pH 14.5 in the current density range (40-225 A $m^{-2}$). Our results show that while it is possible to reach pH values as high as 14.5, this is at the expense of decreasing energy efficiency. In view of technology implementation, coulombic efficiency here is not defined in terms of the main electrode reaction, but with respect to the percentage of the electrochemically produced hydroxide anions that the system can retain in the artificial brine of interest within the cathodic compartment. Important electro-osmotic and classical osmotic effects are observed with the chosen permselective membranes. The most important differences in results produced at varying current density values are observed in the extent of classical osmosis. At lower

applied current density, the flux of water towards the cathodic, more concentrated compartment is larger and hence the species of interest, both cations and hydroxide anions get more diluted. The results are corroborated with a real brine sample for which very similar conclusions were obtained as compared to the artificial brine.

## 2. Experimental

### 2.1. Electrochemical reactor

A three-compartment water electrolyzer was designed and made in-house. The design has previously been reported,[29] and is shown in Figure S1. The main structure was made in acrylic and consisted of three identical compartments with internal dimensions 5 × 20 × 2 cm, and internal volume equal to 200 $cm^3$, separated by two membranes, an anion exchange membrane (AEM) and a cation exchange membrane (CEM), as schematized in Figure 1b. Both membranes were from Membranes International, their characteristics, as specified by the manufacturer, are listed in Table S1. The new membranes were soaked for 24 h in NaCl 5 % before use to allow for their hydration and expansion. After each experiment, they were thoroughly rinsed in de-ionized water and kept in NaCl 5 % solution. Before each experiment, membranes were washed with de-ionized water. The cathode was a stainless-steel wire mesh (4.8 x 19.8 cm) with a stainless-steel sheet metal current collector (4.9 x 19.9 cm). The anode was a titanium mesh electrode coated with an iridium-based mixed metal oxide ($IrO_2/TiO_2$; 65/35 %), with a perpendicular current collector (4.8 × 19.8 cm; 1 mm thickness, Magneto Special Anodes). The distance between electrodes was 2.3 cm. Two plastic meshes were placed between the electrodes and the membranes to avoid direct contact, and to serve as turbulence promotors. All experiments were performed with the same electrochemical reactors, electrodes, and membranes.

All experiments were run in galvanostatic mode, in two electrode configurations, *i.e.* no reference electrode was used. A simple constant current/constant voltage power supply was used (maximum current 5 A, maximum voltage 30 V). Current density values are reported with respect to the geometrical area of the membranes: 0.01 $m^2$ each (the footprint of each electrode was only 2-5% smaller). The chosen current density values were all below the maximum current density reported by the membranes manufacturer (500 A $m^{-2}$). Each experiment was carried out at one unique constant current value. The applied current did not fluctuate more than 0.1 A $m^{-2}$ in any experiment. The cell voltage drop between the two electrodes ($E_{source}$) was monitored directly from the digital screen in the power supply.

Experiments were run in batch recirculation mode at room temperature (20 ± 2) $^{o}$C. All compartments were connected to a dedicated 500 $cm^3$ Schott bottle, that allows for a larger stock of solutions, for operation in batch recirculation mode, and hence forced mass transfer regime. The total initial volumes for anolyte, middle and catholyte were 500 $cm^3$ each. These volumes were constantly recirculated through the cell compartments using a peristaltic pump (flow rate = 17 L $h^{-1}$, PC28 APEMA).

**2.2 Test solutions**

All solutions were prepared with de-ionized water. The anode was always filled with 0.05M $HNO_3$. The middle compartment was filled with 0.07 M HCl in all experiments except those shown in Figure 6, where 0.01 M HCl was used. Both acids from Biopack, analytical grade. The cathodic compartment was filled with a solution made with 3.1 M NaCl (Salinas Grandes, technical grade), which was made alkaline to pH = 13.1 with concentrated NaOH (Biopack) solution. This solution is termed *artificial brine* in the experiments, since its NaCl composition mimics a real brine, and

the pH adjustment simulates pre-treatment as shown in the top left electrolyzer in Figure 1a.

Experiments shown in Figure 7 and denoted as *real brine* were performed on a real or native brine sample coming from a de-identified mining site in northwest Argentina that had been made alkaline (pH = 13.1) in an electrochemical reactor as shown in the top-left corner of Figure 1a in order to remove $Mg^{2+}$ and $Ca^{2+}$. Concentrations in this sample were: $[Li^+]$ = 622 ppm; $[K^+]$ = 5200 ppm; $[Na^+]$ = 116.3 g $L^{-1}$ $[Cl^-]$ = 174.2 g $L^{-1}$; [B] = 919 ppm; $[SO_4^{2-}]$ = 20.0 g $L^{-1}$.

**2.3 Analytical measurements**

0.5 $cm^3$ samples were taken from both the middle and cathodic compartments at regular intervals to measure concentrations evolution with time. Acid-base titration was used to precisely determine $OH^-$ and $H^+$. Chloride anions concentration was determined using Mohr's method. The titrant solution was 0.02 M $AgNO_3$ (Biopack). 5 % $K_2CrO_4$ (Cicarelli) was used as colorimetric indicator.

**2.4. Calculations**

The energy efficiency for the increase in $OH^-$ concentration in the cathodic compartment was defined as:

$$\eta_{OH_n^-} = \frac{([OH^-]_0 * V_0 - [OH^-]_n * V_n) \times F}{\int_0^n i\, dt} \times 100 \qquad \text{(eq. 1)}$$

where $[OH^-]_0$ and $[OH^-]_n$ (M) are concentrations of hydroxide anions, and $V_0$ and $V_n$ (L) are solution volumes in the cathodic compartment, *0* and *n* refer to initial value and value at time *n*, respectively; *F* is the Faraday constant; *i* (A) is the applied current; and *t* (s) is the electrolysis time.

The electrochemical energy consumption per volume of treated brine was calculated according to:

$$E = \int_0^n \frac{E_{source}\, i\, dt}{V_0} \qquad \text{(eq. 2)}$$

where $E_{source}$ $(V)$ is the voltage drop in the cell.

## 3. Results and discussion

In our first report on the ideas schematized in Figure 1a, a native brine was directly fed to the cathodic compartment of a water electrolyzer.[28] That setup showed that it was possible to fully deplete $Mg^{2+}$ and $Ca^{2+}$ cations from the brine. However, $Mg(OH)_2$ and $Ca(OH)_2$ solids were formed within the electrochemical reactor, and hence after batch processing a few litters of brine, the system had to be thoroughly cleaned, to remove the solids from within the reactor.[28] Next, we proposed a modification of that original setup, as shown to the left and centre of figure 1a. A first and unique batch of a native brine is introduced in the cathodic compartment of a first electrochemical reactor (top left of Figure 1a). As the brine is made alkaline, the divalent cations crystallize as hydroxides, as in the original report, and all solids are settled and filtered. The supernatant, which should have reached a pH where multivalent species are no longer present (pH ≈ 13) is introduced in the cathodic compartment of a second electrolyzer (bottom left of Figure 1a). In what is now called STAGE I, the $Li^+$ solution, previously depleted from divalent cations, is made more alkaline (pH > 14). We will call the outflow of this process *super alkaline brine*. This super alkaline brine is used as a precipitating agent and is mixed in an external vessel with native brine that contains divalent cations. Because the external vessel is not an electrochemical reactor, and does not contain any membranes the crystallization of large amounts of solids within that vessel is not an issue. If a stoichiometric amount of $OH^-$ anions is mixed with the native brine, then $Mg(OH)_2$ and $Ca(OH)_2$ will readily crystallize. A small fraction from the supernatant is fed back to STAGE I, in order to prepare more *super*

*alkaline brine*. The larger fraction of the supernatant is ready for further processing (STAGES II and III, to the right of Figure 1a).[30]

There are important differences between this strategy and a chemical alkalinisation (with CaO, or NaOH, for example).[44] Firstly, from a logistic point of view, there is no need for the constant shipping of chemicals to the often remote locations where brine deposits are located. Secondly, chemical alkalinisation makes the brine more complex, $OH^-$ anions come along with more cations. Thirdly, chemical reactants such as CaO or NaOH are most commonly added either as concentrated solutions, or at least in the form of suspensions of solids. Thus, more water is introduced in the system, further diluting $Li^+$ cations, and consuming freshwater, which is usually scarce in these regions, as already pointed out.

Figure 1 shows a schematic representation of the electrolyzer used throughout this work. The chemical species present in the anodic and cathodic compartments limit the possible oxidation and reduction reactions to classical water electrolysis:

At the anode: $$\boldsymbol{H_2O \rightarrow \frac{1}{2}O_2(g) + 2H^+(aq) + 2e^-}$$ (eq. 3)

At the cathode: $$\boldsymbol{2H_2O + 2e^- \rightarrow 2OH^-(aq) + H_2(g)}$$ (eq. 4)

Figure 2a shows the pH increases in the cathodic compartment as the electrolysis advances, an expected behaviour following eq. 4. The electrochemical reactions at the electrodes produce an electrical charge imbalance in both anodic and cathodic compartments, and thus, cations are forced to migrate from the anodic compartment across the CEM to the middle compartment, while anions migrate from the cathodic compartment across the AEM to the middle compartment (ionic migrations schematized in Figure 1b). Because $H^+$ produced at the anode migrate to the middle compartment, there is a marked pH decrease in the middle compartment, as shown in data plotted in Figure 2a.

In Figure 2a no appreciable differences can be seen in the pH evolution with applied current density. Because logarithmic scales might hinder small variations, Figure 2b shows the hydroxide anions' concentrations in the cathodic compartment in molar units. We can observe that $[OH^-]$ seems to increase more slowly for the experiment at 40 A $m^{-2}$, while all other four experiments show indistinguishable results, within experimental error. Figure 2b does not show a linear increase for $[OH^-]$ with the amount of electric charge. Figure 2c is a graph of $\eta_{OH_n^-}$ with the advancement of electrolysis. This variable has been defined to assess the efficiency in conserving the hydroxide anions produced at the cathode within the cathodic compartment. This is not a classical coulombic efficiency. $\eta_{OH_n^-}$ is a coulombic efficiency, in the sense that it quantifies the percentage of electric charge that is used for a defined aim (in here, increasing the pH in the cathodic compartment). $\eta_{OH_n^-}$ is calculated from the start of the electrolysis (eq. 1), and Figure 2c shows that the $\eta_{OH_n^-}$ decreases from 100 % since the start of the process. Thus, when a 60 % efficiency is calculated at 400,000 C $L_{brine}^{-1}$, the instantaneous efficiency at that point is much lower than 60 %.

We should at this point remember that our technological objective is to increase the pH in the cathodic compartment at the lowest possible electric energy cost. Our original strategy was to produce hydroxide anions *in situ* at the cathodic compartment of a water electrolyser to directly crystallize $Mg(OH)_2$ and $Ca(OH)_2$.[28] The large majority of native brines contain a concentration of chloride anions which is no less than 3 M, and pH values below 8.[4–6] Thus, at neutral to mildly alkaline pH values, it is the chloride anions that are almost exclusively responsible for charge transfer across the membrane. Even at pH = 12, chloride anions are still 2 orders of magnitude more concentrated than $\boldsymbol{OH^-}$. Thus, in the original strategy, while inviable from the perspective of solids accumulation within the reactor, the energy efficiency was close to

100 %.[28] Unfortunately, as the concentrations of chloride and $\boldsymbol{OH^-}$ become comparable, both species will participate in charge transfer, which is what Figures 2b and 2c are undoubtedly showing. Thus, while it is certainly possible to continue to increase the pH the coulombic efficiency becomes much lower, the higher the pH. Conversely, the higher the pH of the *super alkaline brine*, the smaller the required amount of this solution that will be necessary to fully deplete the divalent cations in the native brine, and the lower the associated pumping costs.

Figure 3 shows that during the electrolysis important volume changes are produced. The solution volume in the middle compartment increases, while the solution volume in the anodic compartments decrease for all 5 current density values tested. The solution volume in the cathodic compartment decreases for current density values of 50 A $m^{-2}$ or higher, and it increases very slightly for the experiment at 40 A $m^{-2}$. The volume changes can be attributed to three different phenomena: 1- water oxidation and reduction (eq. 3 and 4); 2- electro-osmosis, *i.e.* water molecules being transferred with the migrating ions across the membranes to the middle compartment; and 3- osmotic effects due to different total particle concentrations in each compartment. If we analyse more carefully the magnitude of the volume changes for the different experimental conditions, all three phenomena seem to be combined.

Firstly, water electrolysis cannot explain the volume changes in the middle compartment. Secondly, the magnitude of the volume changes produced by water electrolysis should be current independent, as long as no parasite reactions are produced at the electrodes. These are not expected, considering the composition of the anodic and cathodic solutions, and the chemical resistance of the two electrodes. Thirdly, the volume decrease in the anodic solution should be half of the volume decrease in the cathodic solution, following Faraday's law, which is not the case for any experiment.

Following Faraday's law, water losses of 56 and 28 g should be observed at the cathode and anode, respectively after 300,000 C $L_{brine}^{-1}$ have circulated. In contrast, figures 3a and 3c show volume decreases of 0.463 L and 0.035 L (50 A $m^{-2}$), and 0.230 L and 0.170 L (225 A $m^{-2}$), for anodic and cathodic solutions, respectively. Thus, the ratio of change is not in agreement with Faraday's law, nor are the experimental numbers with expected losses for any of the two extreme current density values (we agree that water mass values do not equate to solution volume changes, but corrections by solution densities could not explain those differences either). Finally, water losses following Faraday's law should be current density independent.

In principle, electro-osmotic effects should also be independent of current, unless a much different current value would trigger the preferential transfer of certain ions over others and the different ions would have different amount of water molecules in their hydration shells.[45] However, there is only one species that can be transferred across the CEM, $H_3O^+$. In turn, only small differences in the amounts of both chloride and hydroxide anions that migrated to the middle compartment were determined. Thus, neither water loss through electrolysis, nor electro-osmosis can explain the different changes in solution volumes as the applied current density is varied.

The explanation seems to be the osmotic effects. Data obtained at different current density values can be directly compared by plotting results as a function of total circulated charge instead of as a function of time. However, experiments with lower applied current density values evidently expand for longer time intervals. Thus, in an experiment that lasts longer, there is more time for water passage from the anodic compartment (roughly constant total particles' concentration of 0.1 M) to the middle compartment (total particle concentration starting at 0.14 M and steadily increasing, see figure 3). In lower current experiments, there is also ample time for large osmotic

effects from the middle to the cathodic compartment. This last osmotic water flow counteracts both the electro-osmotic flow (direction catholyte-middle compartments) and the loss of water by electrochemical reduction.

For example, circulating a total of 200,000 C $L_{brine}^{-1}$ required 5.89 days and 1.03 days at the two extreme current density values of 40 and 225 A $m^{-2}$ (0.4 and 2.25 A effectively applied, membrane area was 0.01 $m^2$). The amount of water that can be transferred driven by classical osmotic effects over a membrane area of 0.01 $m^2$ in a time interval extending up to 6 days is certainly much larger than the amount of water transferred in only 1 day. According to the manufacturer (Table S1) for the membrane size used in these experiments, the water permeability of both AEM and CEM at an applied pressure of 0.352 atm should be not higher than 0.323 mL $h^{-1}$. However, the osmotic pressure developed for concentration differences in the order of 6 M (at the start of the experiment between middle and cathodic compartment) will be over 100 atm,[46,47] and thus the water permeability could increase to values higher than 0.323 mL $h^{-1}$. The precise figures will also vary constantly, since the total number of particles continuously changes in all 3 compartments. The osmotic pressure from the middle to the cathodic compartment will decrease as the electrolysis advances, and therefore the water permeability will also decrease. Over 300,000 C $L_{brine}^{-1}$ are necessary to equilibrate the total amount of particles in the middle and cathodic compartments. Overall, these numbers corroborate our hypothesis that classical osmotic effects are behind the varying changes in solution volumes with applied current density.

Figure 4 shows the evolution of chloride concentration in the cathodic and middle compartments (panels a and b, respectively). The observed behaviour is in line with the evolution of $OH^-$ concentration in the cathodic compartment. Chloride concentration decreases in the cathodic compartment, while it increases in the middle

compartment, but while both changes are monotonous, neither are linear. This is in line with chloride being the major anion responsible for charge transfer at pH ≈ 13, while this role becomes to be shared with $OH^-$ slowly but steadily as the pH increases. Figure 4c shows the evolution of $H^+$concentration in the middle compartment, which is not linear either, due to a certain degree of neutralization as the transfer of $OH^-$ to the middle compartment becomes non-negligible.

It is interesting to observe that while hardly any differences were observed for $OH^-$ concentration evolution in the cathodic compartment for experiments at varying current densities, differences are much more evident for $H^+$ and chloride concentrations in both compartments. In the middle compartment, both chloride and $H^+$ show higher concentrations in the experiments at higher current density values. These correlate well with the volume increases in the middle compartment being lower at higher current densities, *i.e.* the same amount of chloride anions and $H^+$ are transferred to this compartment, but these are mixed in a lower volume of solution.

Figure 5a shows the voltage drop between the electrodes ($\boldsymbol{E_{source}}$) as a function of total circulated charge for the different current density values tested. For the three experiments performed at lower current density values (40-80 A $m^{-2}$) it takes about 10,000 C $L_{brine}^{-1}$ to reach a steady $\boldsymbol{E_{source}}$ value. The voltage drop starts at considerable higher values than the equilibrium value, which is attributed to the low total ionic concentration in the middle compartment (0.07 M HCl). A very quick estimation indicates that after 10,000 C $L_{brine}^{-1}$ the ionic concentration in the middle compartment is multiplied by 2.5 from its initial value (0.17 M HCl), decreasing the solution resistance in the middle compartment from about 1.5 to 0.5 Ω (molar conductivity of HCl is 398.9 and 391.1 S $cm^2$ $mol^{-1}$ at 0.05 M and 0.1 M, respectively[48]). The increase in concentration in the middle compartment will also reduce the membranes' resistance

values, since those resistances are a function of the solution concentration they are in contact with. We also observe that for the two experiments at higher applied current density values (125 and 225 A $m^{-2}$) it takes a larger amount of current density to reach a steady state value for $\boldsymbol{E_{source}}$ (about 100,000 C $L_{brine}^{-1}$ ).

Figure 5b is a current-voltage curve for the overall system. While this is not the classical way of studying electrodialysis type of systems, data in Figure 5b still suggests that a change of mechanism in ionic transport across the system seems to be taking place beyond 125 A $m^{-2}$. Up to that current value, a quasi-ohmic region is observed, where a linear relationship is observed between current and voltage. The effective resistance[49] up to 125 A $m^{-2}$, taking in consideration the resistance of the two membranes, the solution in the bulk of the middle compartment and the depleted and enriched diffusion layers in the vicinity of each membrane, can be estimated at 1.54 Ω, a value that is not far from the summation of the resistance in the bulk of the middle compartment and the resistance of the two membranes (see Table S1). The change in mechanism in ionic transport is likely associated to the observation that it takes longer for the $\boldsymbol{E_{source}}$ vs. circulated charge curve to reach steady state.

Figure 5c is the calculation of the electrical energy consumption for the overall process. It is interesting to observe that there are hardly any changes in the energy consumption of experiments performed at 40 and 50 A $m^{-2}$. Even more striking is the observation that there are hardly any changes in energy consumption in experiments performed at 125 and 225 A $m^{-2}$. This is explained both by the very low $\boldsymbol{E_{source}}$ value difference once a steady $\boldsymbol{E_{source}}$ is reached. In addition, we observe that up to about 76,000 C $L_{brine}^{-1}$ $\boldsymbol{E_{source}}$ is actually higher for the experiment at 125 A $m^{-2}$. These calculations do not take into consideration the energy consumed in solution pumping. In these experiments, the energy consumed in the pumping should be invariable with

applied current density since the same flow rate was used in all experiments. However, optimization of the methodology also entails optimizing the forced mass transfer regime, and thus the required flow rate should be higher when increasing the current density in order to minimize the diffusion layer and avoid water splitting at the membranes.[50,51]

Within experimental error, the same $OH^-$ concentration in the catholyte is reached for the same amount of circulated charge for all current density values between 50 and 225 A $m^{-2}$. Thus, from the perspective of decision making, it would seem that an equilibrium current should be found, between the increased operational costs of working at higher current densities and the lower capital costs of implementing a reduced amount of electrochemical reactors to achieve the same production capacity at higher current density. However, there is still one more variable that should be considered. Figure 3c showed that the volume decrease in the catholyte is larger for the larger current density values. If we recall the original aim behind the technology development, a reduced volume for the aqueous solution containing the valuable raw materials is of great importance. A volume reduction of as much as 20 % can be reached by working at 125 or 225 A $m^{-2}$, as compared to 40 or 50 A $m^{-2}$.

Recalling Figure 1a is helpful to understand why a reduced volume in the catholyte is useful for the consequent processing steps. In the non-electrochemical reactor at the centre of the figure, the super alkaline brine (solution at pH > 14) will be mixed with a native brine containing $Mg^{2+}$ and $Ca^{2+}$. With a Ksp value of $5.61 \times 10^{-12}$,[48] $Mg(OH)_2$ is highly insoluble and will readily crystallize upon addition of the super alkaline brine, around pH ≈ 10.[29] However, the Ksp value of $Ca(OH)_2$ is higher, at $5.02 \times 10^{-6}$,[48] and thus, not only a higher pH will be needed to achieve its crystallization, but also it is desirable to avoid its dilution as much as possible, since

with that Ksp value remnants of $Ca^{2+}$ could remain. Next, after the full depletion of multivalent species, the brine needs to be processed in two further electrochemical systems (Figure 1a, 2 reactors to the right). In those systems, we aim to crystallize $NaHCO_3$ and $Li_2CO_3$, both of which have non-negligible solubilities. Particularly $Li^+$ is already very diluted in native brines (100 – 1500 ppm). Thus, promoting its concentration will help its recovery in subsequent steps. In the overall strategy that we propose in Figure 1a, the largest concentration increase is achieved in the last two electrochemical reactors. This is done by working with a much reduced solution volume in the recovery compartments (catholyte) as compared to the middle compartments.[27] However, the increase in concentrations that can be achieved in electrodialysis type of systems is not unlimited. Thus, up-concentrations achieved in previous steps are certainly welcome.

An experiment was performed with a reduced HCl concentration in the middle compartment, in order to test whether this change would promote a preferential transfer of chloride anions over hydroxides from the catholyte. Results for the two different HCl concentrations (all other conditions were the same) are shown in Figure 6. The most striking difference is the observation that the $OH^-$ concentration in the cathodic compartment is 16 % higher (Figure 6b) in the experiment performed with lower initial HCl concentration in the middle compartment. That higher $OH^-$ concentration translates in a higher efficiency in conserving $OH^-$ in the cathodic compartment (Figure 6c). That is, chloride anions cross the AEM at a slightly higher rate in the experiment with lower HCl concentration (Figure 6d). Surprisingly, there are marked differences in the magnitude of the volume changes in the three compartments, a phenomenon that we tend to associate to regular osmosis, but for which we do not have a closed explanation. As expected, the initial voltage drop between the electrodes was much higher for diluted

HCl in the middle compartment (Figure S2). However, $\boldsymbol{E_{source}}$ drops very quickly and before 10,000 C $L_{brine}^{-1}$ the two values are roughly the same.

We performed one final experiment to see how the electrolytic system would behave with a real brine. Results in Figure 7 show a few differences with experiments performed on the artificial brine. Firstly, the voltage drop is 12 % higher for experiments performed on the artificial brine (Figure 7a). We hypothesize that this could be due to a higher viscosity in the real brine, as well as to the presence of $SO_4^{2-}$ and borates species that will have a more sluggish transport than chlorides and hydroxides. The volume decrease for the solution in the cathodic compartment (Figure 7b) is 10-15 % larger for the artificial brine, a phenomenon for which we do not have yet an explanation. At 216,000 C $L_{brine}^{-1}$, the hydroxide anions concentrations are 1.76 and 2.28 M, in the artificial and native brine respectively (Figure 7d). This difference is not explained by a considerably larger efficiency in retaining hydroxide anions in the cathode (efficiency values are 66.6 and 68.1 % respectively, Figure 7f). The difference stems from the larger volume decrease in the catholyte for the real brine, that results in the same total amount of anions being more concentrated.

## 4. Conclusions

We have studied the competing ion migration between chloride and hydroxide anions across an anion exchange membrane in a water electrolyzer as a function of current density. The most important differences were observed in the magnitude of the changes in the solution volumes in each of the compartments. While water electrolysis and electro-osmotic effects were identified as processes contributing to these changes, only classical osmotic effects are responsible for the differential effects of current density on the volumes. In the range of study, applied current density values from 80-

225 A $m^{-2}$ produce slightly higher $[OH^-]$ concentrations values, although no current density values were identified to produce remarkable changes in the energy efficiency, defined here as the capacity of the system to retain the hydroxide anions within the catholyte solution.

When fully new ore processing technologies are thought, it would be ideal to develop ideas that target for the joint or concomitant harvesting of more than one product from the native ores. Coming back to brines, no by-product is likely to reach the high price of lithium carbonate in the near future, at about 70,000 US$ $tonne^{-1}$ in early 2023. However, the income from selling by-products will always help to cope with the higher energy costs of DLE technologies as compared to the evaporitic technology. The ideas discussed in this work, aim for the production of $Mg(OH)_2$ and $Ca(OH)_2$ as by-products in the overall production of $Li_2CO_3$. We should recall once again that production of by-products results in lesser amounts of waste, and thus, leads to higher sustainability.

While these results are useful to reflect on potential strategies towards technology implementation, a lot of work needs to be undertaken to advance the technology forward. On the positive side, it is a good sign that results on the real brines were comparable to those of the artificial brines. Amongst ideas that must be worked upon is the search for alternative membranes that might be more competitive towards the preferential transfer of chloride vs. hydroxide anions, while showing chemical resistance to high alkalinity. We must acknowledge that diluted solutions in the anodic and middle compartments will lead to high fresh water consumption, something that we should avoid at all costs. In this context, both 0.01 and 0.07 M HCl are very dilute solutions. Thus, experiments on much more concentrated solutions are on schedule.

Finally, variations on the rate of forced mass transport might decrease the depleted diffusion layers in the vicinity of the ion exchange membranes.

**Acknowledgments**

CHDN, WRT and VF are CONICET permanent research fellows. MAM and NAP acknowledge joint doctoral fellowships from DESE-LITHIUM and CONICET, CJOP acknowledges a doctoral fellowship from CONICET. MLV acknowledges a post-doctoral fellowship from CONICET. This work was supported by ANPCyT, AR, grant PICT 2019–1939.

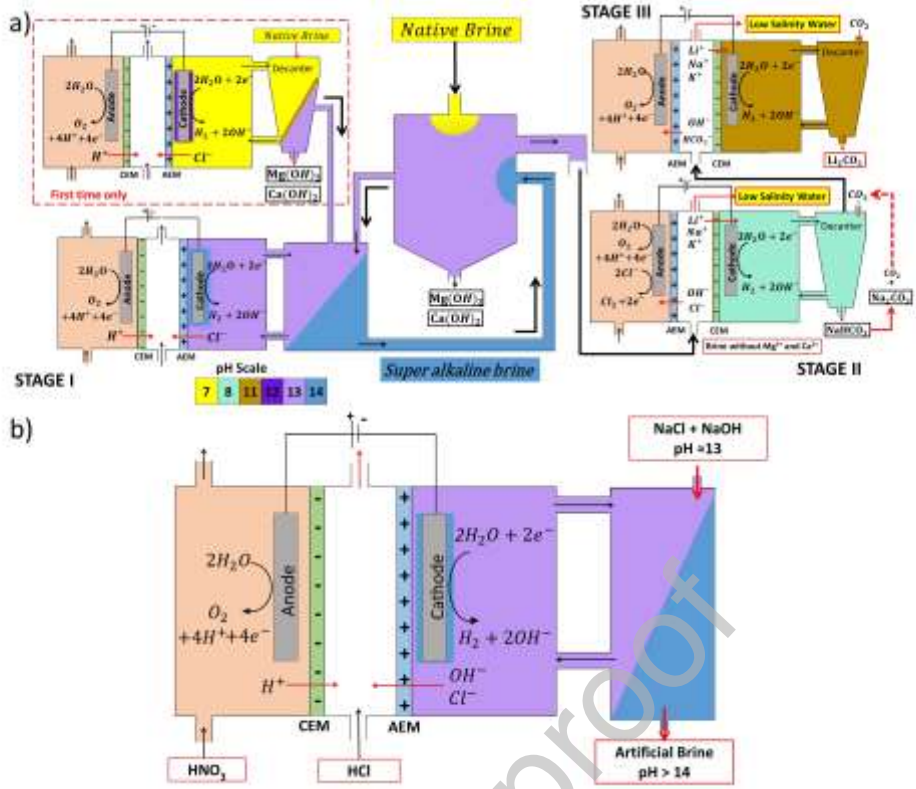


**Figure 1**. **(a)** Schematic representation of the overall electromembrane approach for the joint recovery of $Li_2CO_3$, $Na_2CO_3$, $Mg(OH)_2$, $Ca(OH)_2$, $H_2$, HCl, and low salinity water. Results showing the feasibility of this approach have previously been disclosed in references [26–28,30]. **(b)** Simplified electrochemical setup used in this work.

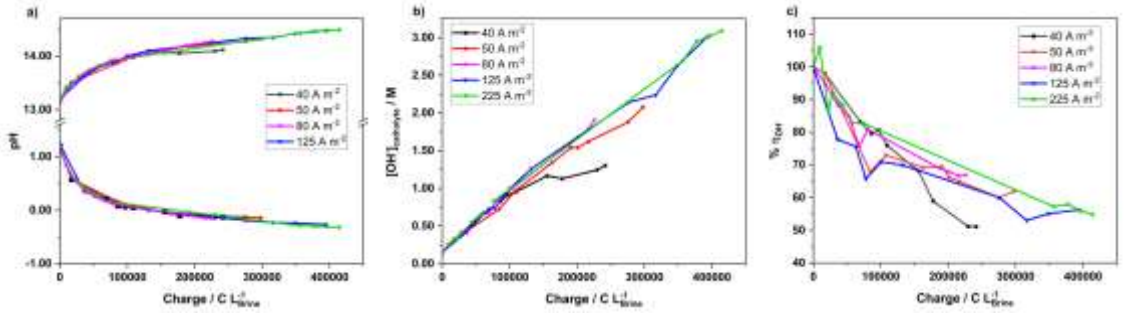


**Figure 2. (a)** pH evolution with the advancement of electrolysis in the cathodic compartment (results starting at pH 13 and up), and in the middle compartment (results starting at pH =1.15 and down). **(b)** Concentration of hydroxide anions in the cathodic compartment (molar units). **(c)** Percentage of the hydroxide anions retained in the cathodic compartment. Experiments at varying current density values as specified in the figure legends. Anodic feed: 0.05 M $HNO_3$. Middle compartment feed: 0.07 M HCl. Cathodic feed: NaCl 3.1M at pH = 13 (adjusted with NaOH).

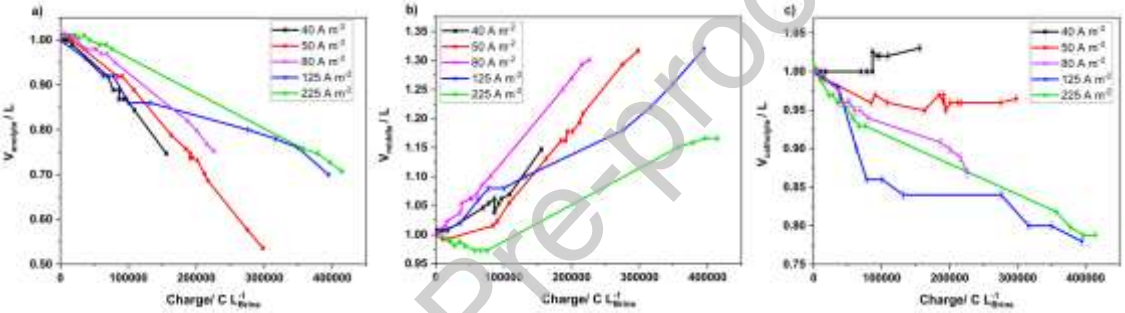


**Figure 3**. Change of volume in the solutions in a) anodic, b) middle and c) cathodic compartments with the advancement of the electrolysis. Experiments at varying current density values as specified in the figure legends. Anodic feed: 0.05 M $HNO_3$. Middle compartment feed: 0.07 M HCl. Cathodic feed: NaCl 3.1M at pH = 13 (adjusted with NaOH).

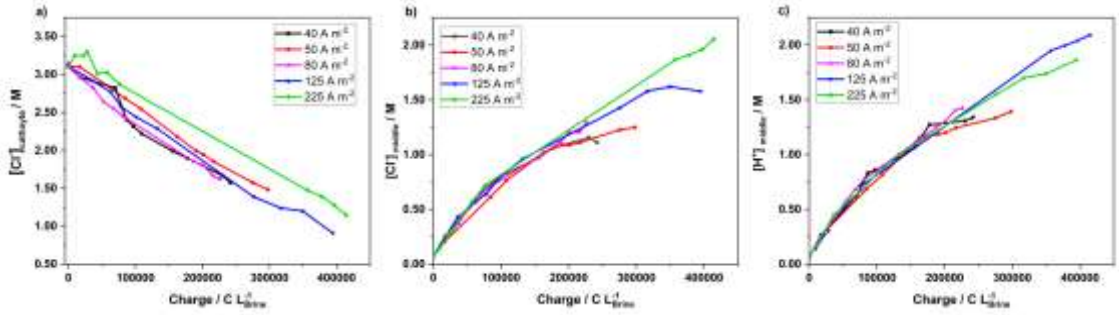


**Figure 4.** Evolution of chloride anions concentrations in the cathodic **(a)** and middle compartments **(b)**. Evolution of proton concentration in the middle compartment **(c)**. Anodic feed: 0.05 M $HNO_3$. Middle compartment feed: 0.07 M HCl. Cathodic feed: NaCl 3.1M at pH = 13 (adjusted with NaOH).

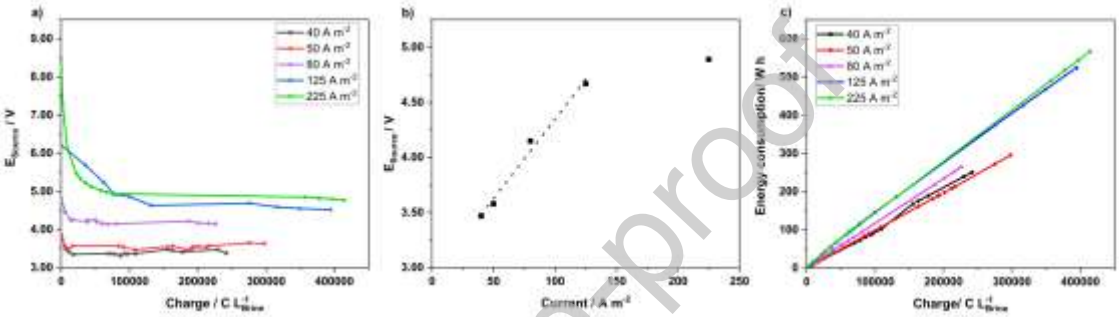


**Figure 5.** Voltage drop ($E_{source}$) between anode and cathode as a function of evolution of the electrolysis **(a)**. $E_{source}$ values (after reaching equilibrium values as a function of the applied current density **(b)**. Energy consumption for the electrolytic process, not including forced mass transfer **(c)**. Anodic feed: 0.05 M $HNO_3$. Middle compartment feed: 0.07 M HCl. Cathodic feed: NaCl 3.1M at pH = 13 (adjusted with NaOH).

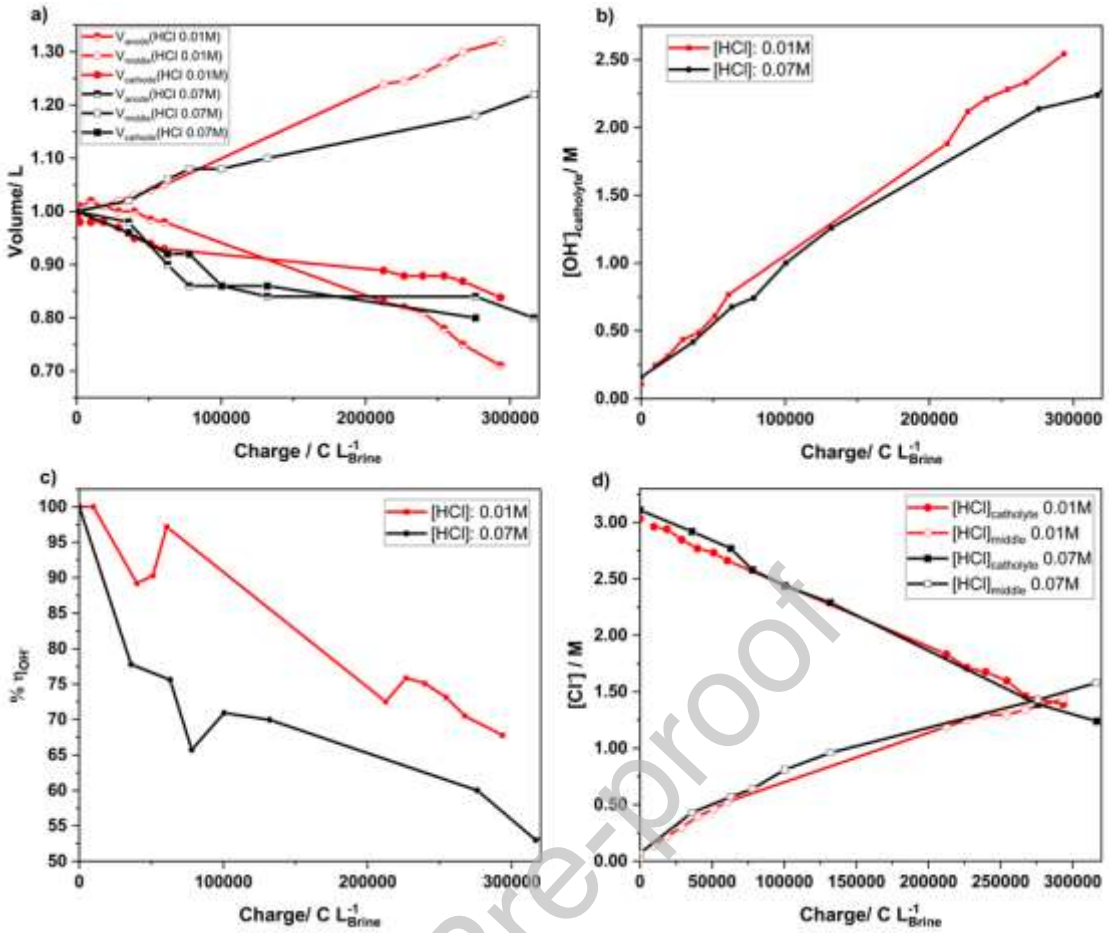


**Figure 6.** Comparison of results for two experiments performed at identical current density values (125 A $m^{-2}$), and the same feeds in cathodic and anodic compartments (0.05 M $HNO_3$ and NaCl 3.1M at pH = 13, adjusted with NaOH, respectively). Varying HCl concentrations in the middle compartment: 0.01 M HCl all red curves, and 0.07 M HCl all black curves. **(a)** Variation in the solution volumes in all three compartments. **(b)** Evolution of hydroxide anions concentrations. **(c)** Percentage of the hydroxide anions retained in the cathodic compartment. **(d)** Evolution of chloride anions concentrations in cathodic and middle compartments.

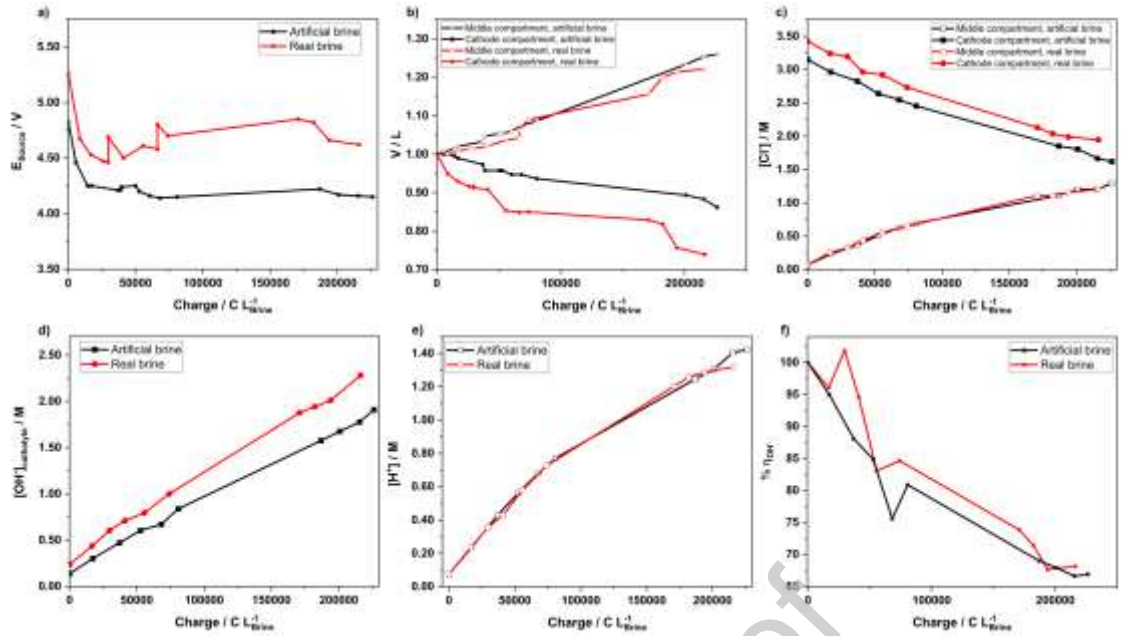


**Figure 7.** Comparison of results for two experiments performed at identical current density values (80 A $m^{-2}$), and the same feeds in anodic and middle compartments (0.05 M $HNO_3$ and HCl 0.07 M respectively). Varying feeds in the cathodic compartment: real brine (see Experimental) all red curves; and NaCl 3.1M at pH = 13, adjusted with NaOH all black curves. **(a)** Voltage drop between the electrodes. **(b)** Variations in the solution volumes in middle and cathodic compartments. Evolution of chloride anions **(c)**, hydroxide anions **(d)** and $H^+$ concentrations **(e)**. Percentage of the hydroxide anions retained in the cathodic compartment **(f)**.

## References

[1] E.A. Olivetti, G. Ceder, G.G. Gaustad, X. Fu, Lithium-Ion Battery Supply Chain Considerations: Analysis of Potential Bottlenecks in Critical Metals, Joule. 1 (2017) 229–243. https://doi.org/10.1016/j.joule.2017.08.019.

[2] L. Trahey, F.R. Brushett, N.P. Balsara, G. Ceder, L. Cheng, Y.-M. Chiang, N.T. Hahn, B.J. Ingram, S.D. Minteer, J.S. Moore, V. Srinivasan, G.W. Crabtree, Energy storage emerging: A perspective from the Joint Center for Energy Storage Research, Proc. Natl. Acad. Sci. U. S. A. 117 (2020) 12550–12557. https://doi.org/10.1073/pnas.1821672117.

[3] C.B. Tabelin, J. Dallas, S. Casanova, T. Pelech, G. Bournival, S. Saydam, I. Canbulat, Towards a low-carbon society: A review of lithium resource availability, challenges and innovations in mining, extraction and recycling, and future perspectives, Miner. Eng. 163 (2021) 106743. https://doi.org/10.1016/J.MINENG.2020.106743.

[4] D.E. Garrett, Handbook of Lithium and Natural Calcium Chloride, 2004. https://doi.org/10.1016/B978-0-12-276152-2.X5035-X.

[5] M.L. Vera, W.R. Torres, C.I. Galli, A. Chagnes, V. Flexer, Environmental impact of direct lithium extraction from brines, Nat. Rev. Earth Environ. 4 (2023) 149–165. https://doi.org/10.1038/s43017-022-00387-5.

[6] B. Sanjuan, B. Gourcerol, R. Millot, D. Rettenmaier, E. Jeandel, A. Rombaut, Lithium-rich geothermal brines in Europe: An up-date about geochemical characteristics and implications for potential Li resources, Geothermics. 101 (2022) 102385. https://doi.org/10.1016/J.GEOTHERMICS.2022.102385.

[7] E.J.M. Dugamin, A. Richard, M. Cathelineau, M.-C. Boiron, F. Despinois, A. Brisset, Groundwater in sedimentary basins as potential lithium resource: a global prospective study, Sci. Rep. 11 (2021) 21091. https://doi.org/10.1038/s41598-021-99912-7.

[8] G.M. Mudd, Sustainable/responsible mining and ethical issues related to the Sustainable Development Goals, Geol. Soc. London, Spec. Publ. 508 (2021) 187 LP – 199. https://doi.org/10.1144/SP508-2020-113.

[9] R. Pell, L. Tijsseling, K. Goodenough, F. Wall, Q. Dehaine, A. Grant, D. Deak, X. Yan, P. Whattoff, Towards sustainable extraction of technology materials through integrated approaches, Nat. Rev. Earth Environ. 2 (2021) 665–679. https://doi.org/10.1038/s43017-021-00211-6.

[10] W.T. Stringfellow, P.F. Dobson, Technology for the Recovery of Lithium from Geothermal Brines, Energies. 14 (2021). https://doi.org/10.3390/en14206805.

[11] X. Zhao, S. Yang, Y. Hou, H. Gao, Y. Wang, D.A. Gribble, V.G. Pol, Recent progress on key materials and technical approaches for electrochemical lithium extraction processes, Desalination. 546 (2023) 116189. https://doi.org/10.1016/J.DESAL.2022.116189.

[12] L. Wu, C. Zhang, S. Kim, T.A. Hatton, H. Mo, T.D. Waite, Lithium recovery using electrochemical technologies: Advances and challenges, Water Res. 221 (2022) 118822. https://doi.org/10.1016/J.WATRES.2022.118822.

[13] E.J. Calvo, Direct Lithium Recovery from Aqueous Electrolytes with Electrochemical Ion Pumping and Lithium Intercalation, ACS Omega. 6 (2021) 35213–35220. https://doi.org/10.1021/acsomega.1c05516.

[14] A. Khalil, S. Mohammed, R. Hashaikeh, N. Hilal, Lithium recovery from brine: Recent developments and challenges, Desalination. 528 (2022) 115611. https://doi.org/https://doi.org/10.1016/j.desal.2022.115611.

[15] D.B. Agusdinata, H. Eakin, W. Liu, Critical minerals for electric vehicles: A telecoupling review, Environ. Res. Lett. 17 (2022). https://doi.org/10.1088/1748-9326/ac4763.

[16] D.B. Agusdinata, W. Liu, S. Sulistyo, P. LeBillon, J. Wegner, Evaluating sustainability impacts of critical mineral extractions: Integration of life cycle sustainability assessment and SDGs frameworks, J. Ind. Ecol. (2022). https://doi.org/10.1111/jiec.13317.

[17] M.A. Marazuela, E. Vázquez-Suñé, C. Ayora, A. García-Gil, Towards more sustainable brine extraction in salt flats: Learning from the Salar de Atacama, Sci. Total Environ. 703 (2020) 135605. https://doi.org/10.1016/j.scitotenv.2019.135605.

[18] J.F. Song, L.D. Nghiem, X.-M. Li, T. He, S. Jianfeng, L.D. Nghiem, X.-M. Li, Lithium extraction from Chinese salt-lake brines: Opportunities, challenges, and future outlook, Environ. Sci. Water Res. Technol. 3 (2017) 593–597. https://doi.org/10.1039/C7EW00020K.

[19] H. Brody, Building a circular economy, Nature. 611 (2022) S1. https://doi.org/10.1038/d41586-022-03643-2.

[20] P.H.-M. Kinnunen, A.H. Kaksonen, Towards circular economy in mining: Opportunities and bottlenecks for tailings valorization, J. Clean. Prod. 228 (2019) 153–160. https://doi.org/10.1016/j.jclepro.2019.04.171.

[21] A.P.M. Velenturf, S.A. Archer, H.I. Gomes, B. Christgen, A.J. Lag-Brotons, P. Purnell, Circular economy and the matter of integrated resources, Sci. Total Environ. 689 (2019) 963–969. https://doi.org/10.1016/j.scitotenv.2019.06.449.

[22] S. Singh, L.B. Sukla, S.K. Goyal, Mine waste & circular economy, in: Mater. Today Proc., 2020: pp. 332–339. https://doi.org/10.1016/j.matpr.2020.01.616.

[23] I. Ihsanullah, J. Mustafa, A.M. Zafar, M. Obaid, M.A. Atieh, N. Ghaffour, Waste to wealth: A critical analysis of resource recovery from desalination brine, Desalination. 543 (2022) 116093. https://doi.org/10.1016/J.DESAL.2022.116093.

[24] O. Ogunbiyi, J. Saththasivam, D. Al-Masri, Y. Manawi, J. Lawler, X. Zhang, Z. Liu, Sustainable brine management from the perspectives of water, energy and mineral recovery: A comprehensive review, Desalination. 513 (2021) 115055. https://doi.org/10.1016/j.desal.2021.115055.

[25] A. Kumar, G. Naidu, H. Fukuda, F. Du, S. Vigneswaran, E. Drioli, J.H. Lienhard, Metals Recovery from Seawater Desalination Brines: Technologies, Opportunities, and Challenges, ACS Sustain. Chem. Eng. 9 (2021) 7704–7712. https://doi.org/10.1021/acssuschemeng.1c00785.

[26] C.H. Diaz Nieto, K. Rabaey, V. Flexer, Membrane electrolysis for the removal of Na+ from brines for the subsequent recovery of lithium salts, Sep. Purif. Technol. 252 (2020) 117410. https://doi.org/10.1016/j.seppur.2020.117410.

[27] W.R. Torres, C.H. Díaz Nieto, A. Prévoteau, K. Rabaey, V. Flexer, Lithium carbonate recovery from brines using membrane electrolysis, J. Memb. Sci. 615 (2020) 118416. https://doi.org/10.1016/j.memsci.2020.118416.

[28] C.H. Díaz Nieto, N.A. Palacios, K. Verbeeck, A. Prévoteau, K. Rabaey, V. Flexer, Membrane electrolysis for the removal of Mg2+ and Ca2+ from lithium rich brines, Water Res. 154 (2019) 117–124. https://doi.org/10.1016/j.watres.2019.01.050.

[29] C.H. Díaz Nieto, J.A. Kortsarz, M.L. Vera, V. Flexer, Effect of temperature, current density and mass transport during the electrolytic removal of magnesium ions from lithium rich brines, Desalination. 529 (2022) 115652. https://doi.org/10.1016/j.desal.2022.115652.

[30] M.L. Vera, C.J.O. Palacios, C.H. Díaz Nieto, N.A. Palacios, N. Di Carlantonio, F.G. Luna, W.R. Torres, V. Flexer, A strategy to avoid solid formation within the reactor during magnesium and calcium electrolytic removal from lithium-rich brines, J. Solid State Electrochem. (2022). https://doi.org/10.1007/s10008-022-05219-6.

[31] X.-J.J. Pan, Z.-H.H. Dou, D.-L.L. Meng, X.-X.X. Han, T.-A.A. Zhang, Electrochemical separation of magnesium from solutions of magnesium and lithium chloride, Hydrometallurgy. 191 (2020) 105166. https://doi.org/https://doi.org/10.1016/j.hydromet.2019.105166.

[32] J. Wang, X. Tang, X. Cheng, J. Xing, H. Wang, G. Li, H. Liang, In-situ crystallization generated by CEM electrolysis for NF concentrate softening along with the alleviation of ceramic membrane fouling, Desalination. 516 (2021) 115243. https://doi.org/10.1016/J.DESAL.2021.115243.

[33] X.J. Pan, Z.H. Dou, T.A. Zhang, D.L. Meng, Y.Y. Fan, Separation of metal ions and resource utilization of magnesium from saline lake brine by membrane electrolysis, Sep. Purif. Technol. 251 (2020) 117316. https://doi.org/10.1016/J.SEPPUR.2020.117316.

[34] Q. Li, H. Liu, B. He, W. Shi, Y. Ji, Z. Cui, F. Yan, Y. Mohammad, J. Li, Ultrahigh-efficient separation of Mg2+/Li+ using an in-situ reconstructed positively charged nanofiltration membrane under an electric field, J. Memb. Sci. 641 (2022) 119880. https://doi.org/https://doi.org/10.1016/j.memsci.2021.119880.

[35] X.-Y. Nie, S.-Y. Sun, Z. Sun, X. Song, J.-G. Yu, Ion-fractionation of lithium ions from magnesium ions by electrodialysis using monovalent selective ion-exchange membranes, Desalination. 403 (2017) 128–135. https://doi.org/https://doi.org/10.1016/j.desal.2016.05.010.

[36] P.-Y. Ji, Z.-Y. Ji, Q.-B. Chen, J. Liu, Y.-Y. Zhao, S.-Z. Wang, F. Li, J.-S. Yuan, Effect of coexisting ions on recovering lithium from high Mg2+/Li+ ratio brines by selective-electrodialysis, Sep. Purif. Technol. 207 (2018) 1–11. https://doi.org/https://doi.org/10.1016/j.seppur.2018.06.012.

[37] D. Ding, A. Yaroshchuk, M.L. Bruening, Electrodialysis through nafion membranes coated with polyelectrolyte multilayers yields >99% pure monovalent ions at high recoveries, J. Memb. Sci. 647 (2022) 120294. https://doi.org/https://doi.org/10.1016/j.memsci.2022.120294.

[38] J. Chen, J. Wang, Z.Y. Ji, Z. Guo, P. Zhang, Z. Huang, Electro-nanofiltration membranes with high Li+/Mg2+ selectivity prepared via sequential interfacial polymerization, Desalination. 549 (2023) 116312. https://doi.org/10.1016/J.DESAL.2022.116312.

[39] K. Shen, Q. He, Q. Ru, D. Tang, T.Z. Oo, M. Zaw, N.W. Lwin, S.H. Aung, S.C. Tan, F. Chen, Flexible LATP composite membrane for lithium extraction from seawater via an electrochemical route, J. Memb. Sci. 671 (2023) 121358. https://doi.org/10.1016/J.MEMSCI.2023.121358.

[40] X. juan Pan, Z. he Dou, T. an Zhang, D. liang Meng, X. xiu Han, Basic study on direct preparation of lithium carbonate powders by membrane electrolysis, Hydrometallurgy. 191 (2020) 105193. https://doi.org/https://doi.org/10.1016/j.hydromet.2019.105193.

[41] M. Ejeian, A. Grant, H.K. Shon, A. Razmjou, Is lithium brine water?, Desalination. 518 (2021) 115169. https://doi.org/10.1016/J.DESAL.2021.115169.

[42] D. Pletcher, F.C. Walsh, Industrial Electrochemistry, Springer Netherlands, 1990.

[43] F.C. Walsh, D. Pletcher, Electrochemical Engineering and Cell Design, in: Dev. Electrochem. Sci. Inspired by Martin Fleischmann, 2014: pp. 95–111. https://doi.org/10.1002/9781118694404.ch6.

[44] C. Morgante, F. Vassallo, D. Xevgenos, A. Cipollina, M. Micari, A. Tamburini, G. Micale, Valorisation of SWRO brines in a remote island through a circular approach: Techno-economic analysis and perspectives, Desalination. 542 (2022) 116005. https://doi.org/10.1016/J.DESAL.2022.116005.

[45] B. Tansel, Significance of thermodynamic and physical characteristics on permeation of ions during membrane separation: Hydrated radius, hydration free energy and viscous effects, Sep. Purif. Technol. 86 (2012) 119–126. https://doi.org/10.1016/j.seppur.2011.10.033.

[46] C.F. Baspineiro, J. Franco, V. Flexer, Potential water recovery during lithium mining from high salinity brines, Sci. Total Environ. 720 (2020) 137523. https://doi.org/10.1016/j.scitotenv.2020.137523.

[47] E. Nagy, Chapter 21 - Pressure-Retarded Osmosis (PRO) Process, in: E.B.T.-B.E. of M.T.T. a M.L. (Second E. Nagy (Ed.), Elsevier, 2019: pp. 505–531. https://doi.org/https://doi.org/10.1016/B978-0-12-813722-2.00021-2.

[48] D.R. Lide, CRC Handbook of Chemistry and Physics, 2005.

[49] K.S. Barros, M.C. Martí-Calatayud, T. Scarazzato, A.M. Bernardes, D.C.R. Espinosa, V. Pérez-Herranz, Investigation of ion-exchange membranes by means of chronopotentiometry: A comprehensive review on this highly informative and multipurpose technique, Adv. Colloid Interface Sci. 293 (2021) 102439. https://doi.org/10.1016/J.CIS.2021.102439.

[50] R. Simons, Water splitting in ion exchange membranes, Electrochim. Acta. 30 (1985) 275–282. https://doi.org/10.1016/0013-4686(85)80184-5.

[51] O.A. Rybalkina, K.A. Tsygurina, E.D. Melnikova, G. Pourcelly, V. V. Nikonenko, N.D. Pismenskaya, Catalytic effect of ammonia-containing species on water splitting during electrodialysis with ion-exchange membranes, Electrochim. Acta. 299 (2019) 946–962. https://doi.org/10.1016/J.ELECTACTA.2019.01.068.

# Credit author

**CHDN:** Conceptualization, Data Curation, Formal Analysis, Investigation, Methodology, Supervision.

**MAM:** Investigation, Visualization.

**CJOP:** Investigation, Visualization.

**NAP:** Investigation; Conceptualization.

**WRT:** Investigation; Conceptualization.

**MLV**: Investigation; Conceptualization.

**VF**: Conceptualization, Methodology, Formal Analysis, Writing-original draft, Writing-review & editing, Supervision, Funding acquisition.



# Graphical Abstract

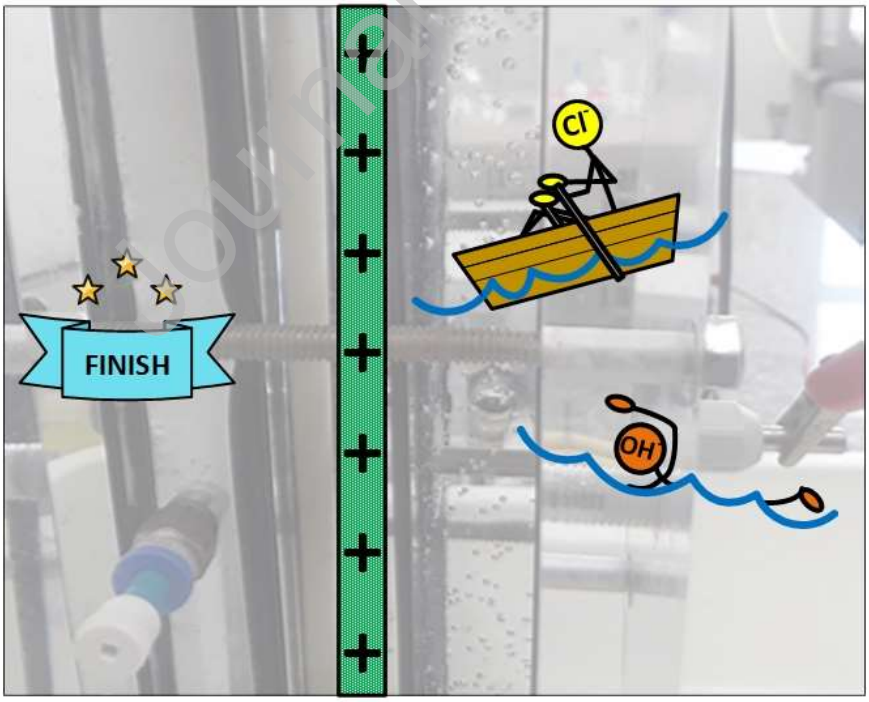

**Declaration of interests**

☒ The authors declare that they have no known competing financial interests or personal relationships that could have appeared to influence the work reported in this paper.

☐ The authors declare the following financial interests/personal relationships which may be considered as potential competing interests: